# STUDY OF SH-SY5Y CANCER CELLS RESPONSE TO IONIZING RADIATION BY VIBRATIONAL SPECTROSCOPIES.

Lorenzo Manti
Valerio Riccardi,
Dipartimento di Fisica,
Università "Federico II",
Napoli, Italy
manti@na.infn.it
ricciardi@na.infn.it

Giuseppe Perna,
Maria Lasalvia,
Vito Capozzi
Dipartimento di Medicina Clinica e Sperimentale,
Università di Foggia,
Foggia, Italy
giuseppe.perna@unifg.it
maria.lasalvia@unifg.it
vito.capozzi@unifg.it

Ines Delfino
Dipartimento di Scienze Ecologiche e Biologiche,
Università della Tuscia
Viterbo, Italy
delfino@unitus.it

Marianna Portaccio,
Maria Lepore
Dipartimento di Medicina Sperimentale,
Università della Campania "Luigi Vanvitelli",
Napoli, Italy
portaccio@unicampania.it
lepore@unicampania.it

**Abstract**
Raman and Fourier-Transform infrared micro-spectroscopies have been used to study neuroblastoma SH-SY5Y cells irradiated with different doses of X-ray. Results show that radiation-induced changes in structure, protein, nucleic acid, lipid, and carbohydrate content can be detected.

**Keywords:**
Single human intact cells; micro-Raman spectroscopy; FT-infrared spectroscopy; x-ray radiation; radiation dose effects.

## 1 Introduction

Continued investigation on radiation interactions with cells and tissues is necessary to increase our knowledge on outstanding radiobiological issues such as the variation in patient radiosensitivity, the inability to monitor a patient's radioresponse during the course of an extended treatment, and the failure of current models to predict cell survival or tumour control at single high doses. Vibrational techniques, as Raman and Fourier-Transform infrared microspectroscopies (μ-RS and μ-FTIR), can be particularly useful in investigating the chemical changes induced in structure, protein, nucleic acid, lipid, and carbohydrate content of cells. μ-RS and μ-FTIR studies of cellular biomolecules have reached considerable attention [Puppels et 1990, Hamada et al 2008, Sakudo 2016, Baker et al 2014]. In the last years, μ-FTIR and μ-RS has also been applied for investigating some kinds of human cells exposed to X-ray [Qi et al 2009, Risi et al 2011, Matthews et al 2011, Delfino et al 2015, Meade et al 2010 ]. The aim of this work is to employ both μ-RS and μ-FTIR for investigating structural and bio-chemical modifications in *in vitro* neuroblastoma SH-SY5Y cells fixed immediately after (t0-cells) and 24 h after irradiation (t24h-cells). This enables to study both the effects of the irradiation and the efficacy of the recovery process of the cells. The analysis of vibrational spectra by simple regression analysis and by multivariate methods on the whole spectra and on selected ranges of the spectra has allowed us to evidence the subtle variations in the Raman fingerprints of proteins, lipids and nucleic acids due to x-ray radiation expositions. Particular attention has also been paid to the comparison of results from t0-cells and t24h-cells.

## 2 Materials and Methods

Neuroblastoma SH-SY5Y cells were grown on polylysine-coated glass coverslips (22 ×22 × 0.17 $mm^3$) in α-MEM medium at 37°C, 5% CO2. Polylysine improves the adhesion of cells on the glass coverslips. The concentration of cells was around 2 × $10^5$ cells/$cm^2$ such that the cells were not confluent but intercellular spaces were left for measuring the background signal. A STABILIPLAN machine (Siemens, Munich, Germany) was used for X-ray irradiation. X-rays (250 kVp) were produced by a Thomson tube (TR 300F) and filtered by 1-mm-thick Cu foil. Cellular samples were exposed to various doses of x-rays at a dose rate of 0.95 Gy/min. In particular, cells exposed to 2, 4, 6, 8 and 10 Gy were investigated together with nonexposed cells (0 Gy). After the exposure, a set of cells was immediately fixed in paraformaldehyde 3.7%. Another set (maintained in α-MEM medium at 37°C, 5% CO2) was allowed to recover for 24 h after the end of the exposure process and was then fixed in paraformaldehyde 3.7%.

μ-FTIR spectra were obtained by using a Perkin Elmer Spectrum One FTIR spectrometer equipped with a

Perkin Elmer Multiscope system infrared microscope (Mercury Cadmium Telluride detector). Spectral acquisitions were performed in transreflection mode on neuroblastoma cells grown on Mirr-IR microscope slides. The background spectrum was collected from the reflective surface in the absence of the sample. A sampling spot on the surface was selected through an objective (10X optical). All spectra were collected using 16 scans in the range from 4000 to 600 $cm^{-1}$ with a 4 $cm^{-1}$ spectral resolution. The spectra were preliminarily analyzed using the application routines provided by the software package controlling the whole data acquisition system.

Raman spectra were recorded by means of a micro-Raman spectrometer (LabRam, Jobin-Yvon Horiba), by using an Argon laser operating at $\lambda = 514nm$. The laser beam was focused on samples by an Olympus optical microscope with a 100×oil immersion objective (with numerical aperture, NA = 1.4). To eliminate external contributions the background signal (from the glass coverslip and PBS solution) recorded for each coverslip from a region where no cells were present was subtracted. Fluorescence contribution was also subtracted using a fifth order polynomial fit with initial points manually selected.

Deconvolution procedure, simple regression analysis and multivariate methods as described in Ref.[Delfino et al, 2015] were used for analyzing the spectra.

## 3 Results and Discussion

In Figure 1 the infrared spectra of SH-SY5Y cells in the wavenumber regions of interest are reported together with results of the deconvolution procedure.

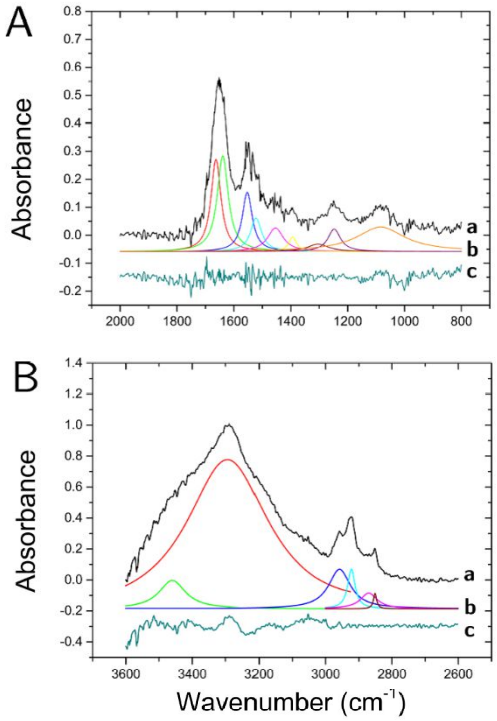


Figure 1. SH-SY5Y cells average infrared spectra and deconvolution analysis of peaks with Lorentzian curves

In Table 1 details about the tentative assignment of peaks that are present in infrared spectra as obtained by deconvolution procedure are reported. Contribution from proteins, lipids and DNA/RNA are clearly evidenced.

In Figure 2 the infrared spectra of cells exposed to different X-ray doses are shown. It can be noticed that differences are present in various regions of the spectra, including the ones of amide I and lipid fingerprints.

| **Peak ($cm^{-1}$)** | **Assignments** |
|---|---|
| 3293 | Amide A (N-H str.) (p) |
| 2957 | $CH_3$ asym. str. (p)<br>$CH_3$ asym. str. (l) |
| 2922 | $CH_2$ asym. str.(l) |
| 2869 | $CH_3$ sym. str. (p)<br>$CH_3$ sym. str. (l) |
| 2850 | $CH_2$ sym. str.(l) |
| 1663 | Amide I (α-helix) (p) |
| 1639 | Amide II (β-sheets) (p) |
| 1553 | Amide II (α-helix) (p) |
| 1522 | Amide II (β-sheets) (p) |
| 1454 | $CH_3$asym. ben.<br>$CH_2$ sc.(p)<br>$CH_3$asym. ben.(l)<br>$CH_2$ sc (l) |
| 1393 | $COO^-$ sym. str.(p)<br>$COO^-$ sym. str. (l) |
| 1304 | Amide III (p) |
| 1247 | $PO_2^-$asym. str.(d) |
| 1084 | $PO_2^-$ sym. str. |

Table 1. Infrared peaks, with assignments in accordance with the data reported in the literature; abbreviation: sym=symmetric, asym=asymmetric, str, stretching, ben, bending, sc, scissoring, p, proteins; d, DNA/RNA; l, lipids.

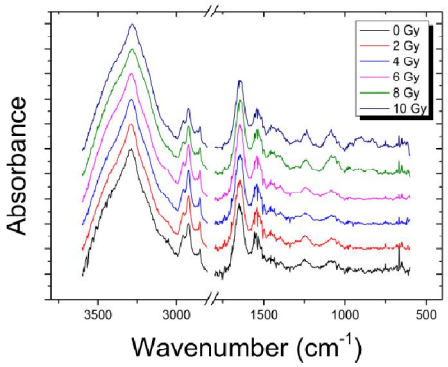


Figure 2. Comparison of average FTIR spectra in the region [3600-600 $cm^{-1}$] of the control cells (0 Gy; t=0) and irradiated cells (2, 4, 6, 8, 10 Gy; t=0).

In particular, significant changes in the positions of several peaks and in the amide I structure have been obtained. The changes in the amide I structure indicate modifications in the secondary structure of protein content of radioexposed cells.

| Peak ($cm^{-1}$) | Assignments |
|---|---|
| 2980 | $CH_3$ asym. str. (p) (l) |
| 2938 | $CH_3$ sym. str. (p) (l) |
| 2885 | $CH_2$ sym. str. (l) (p) |
| 2858 | $CH_2$asym. str. (p)(l) |
| 1661 | Amide I (α -helix, β -sheets, coil) (p)<br>C=C sym. str. |
| 1608 | Phenylanine<br>/Tyrosine C=C (p) |
| 1575 | Adenine, Guanine (d) |
| 1452 | $CH_2/CH_3$ ben. (p)<br>CH def.(p) (l), $CH_2$sc. (l) CH def (l) |
| 1338 | $CH_2$tw., CH def. (p)<br>Adenine, Guanine (d), CH def. (c) |
| 1309 | Amide III (p)<br>Adenine, Cytosine (d), $CH_2$tw (l) |
| 1297 | $CH_2$tw. (l) |
| 1256 | Amide III (α -helix) (p)<br>$CH_2$def. (l) |
| 1248 | Amide III (β -sheets) (p)<br>Tymine (d) |
| 1235 | Amide III (random coil) (p) |
| 1204 | Tryptopan/Tyrosine (p)<br>/Phenylanine (p)<br>CH sym. str. (p) CH ben.(p) |
| 1168 | Phenylanine/Tyrosine (p)<br>CH ben. (p) |
| 1123 | CN sym. str. (p)<br>CC asym. str. (l), CO str. (d) |
| 1090 | $PO_2^-$sym. str. (d)<br>CC chain sym. str. (l)<br>C0 , C=C str. (c) |
| 1027 | Phenylanine CH in-p. ben. |
| 998 | Phenylanine sym. ringbr. |
| 973 | CC sym. str., β -sheets (p)<br>$PO_3^{2-}$sym. str. (d)<br>CH ben.(l) |
| 955 | $CH_3$def. (p) (l) |
| 932 | CC sym. str., α -helix (p)<br>COC glycos. bond (c) |
| 886 | cDNA (d)<br>CC N sym. str (l)<br>COC ring,$C_1-C_2$ str. (c) |
| 849 | Tyrosine ring br.<br>Proline CC str. |
| 823 | Tyrosine o-p. br. (p)<br>$PO_2^-$asym. str (l) |
| 778 | Cytosine/Tymine<br>/Uracil ring br. (d) |

Table 2. Raman peaks and relative assignments in agreement with the data reported in the literature. Abbreviation: sym,symmetric; asym,asymmetric; str, stretching; br, breathing; tw,twist; in-p,in-plane;o-p,out-of-plane; ben,bending; def, deformation; sc,scissoring; p, proteins; d, DNA/RNA; l, lipids, c, carbohydrates.

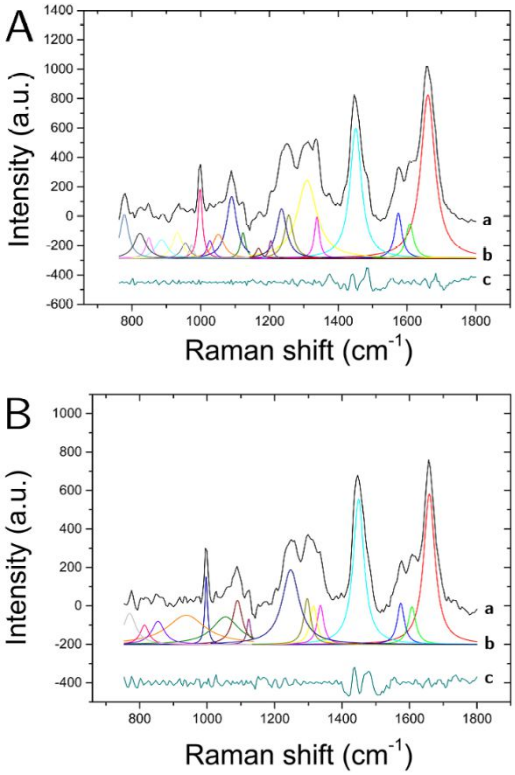


Figure 3 SH-SY5Ycells average Raman spectra of the nucleus (A) (0 Gy; t=0) and the membrane (B) in the [700-1800 $cm^{-1}$] range.

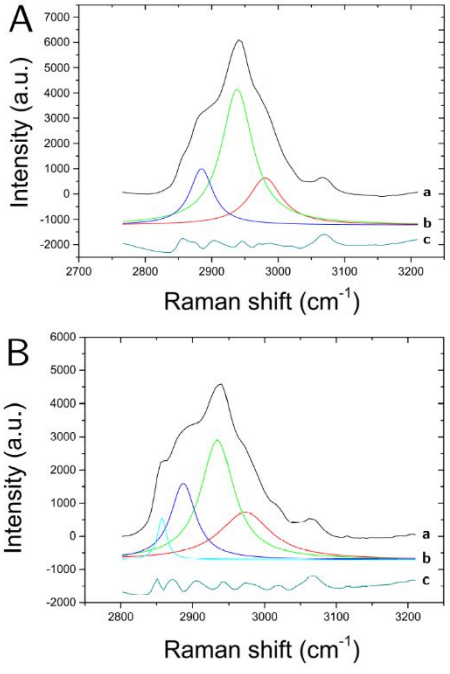


Figure 4 SH-SY5Ycells average Raman spectra of the nucleus (A) (0 Gy; t=0) and the membrane (B) in the [2800 - 3200 $cm^{-1}$] range.

The collecting geometry adopted for μ-RS measurements allowed us to obtain spectra related mainly to the nucleus and membrane regions of the cells. The spectra for the two cell regions and for the

two ranges of wavenumber shifts of interest are reported in Figure 3 and 4. As expected a great number of peaks is present in the spectra; their positions are listed in Table 2 together with their assignments. Using the above-mentioned deconvolution procedure, the spectra have been analyzed in terms of Lorentzian shaped vibration modes. This analysis has allowed us to single out the peak positions of the main cell components: DNA nitrogeneous bases, aminoacids, amide I, amide III and lipids, for further details see Table 2. The same peaks are present in the Raman spectra of control and exposed cells. In some cases, the peaks are significantly shifted (i.e, a wavenumber shift greater than the spectral resolution is observed). In order to highlight the differences occurring between control and exposed cell spectra, different peak intensity ratio have been examined. In particular, $I_{998}/I_{1452}$, $I_{1027}/I_{1452}$, $I_{1608}/I_{1452}$,$I_{1235}/I_{1452}$, $I_{1309}/I_{1452}$ ratios show different values when spectra from the samples exposed at different doses are considered, which is likely to indicate aminoacids and nitrogenous DNA bases fragmentation. Moreover, $I_{778}/I_{1452}$ and $I_{1090}/I_{1452}$ ratios (where the peak at 778 $cm^{-1}$and 1090 $cm^{-1}$a re relative to the O-P-O and O=P=O stretching, respectively) decrease after exposition suggesting an increase of the DNA rigidity, probably related to a molecular crosslink, which makes DNA structure more compact. Further analysis using univariate and multivariate analysis is still in progress.

## 4 Conclusion

The presented analysis of vibrational spectra from irradiatedSH–SY5Y neuroblastoma cells confirmed that they show significant differences compared to the spectra of control cells. In particular, Raman measurements were performed by using experimental conditions well suited to record spectra from intact cells. Our investigation confirms a good sensitivity of the vibrational techniques to detect the chemical changes induced by x-ray radiation on fixed cells. Hence, these techniques could be useful in the field of radiotherapy to monitor the minimal doses sufficient to lethally damage the cancer cells, thus reducing the risk of providing the patient with an excess of dose that could lead to damage of surrounding healthy cells.

## References


Puppels J. R. et al (1990).
Studying single living cells and chromosomes by confocal Raman microspectroscopy. Nature, 347, pp.301–303.

Hamada K., Fujita K., Smith N. I., Kobayashi M., Inouye Y., Kawata S. (2008)
Raman microscopy for dynamic molecular imaging of living cells ", J. Biomed. Opt. 13, 044027

Sakudo A (2016)
Near-infrared spectroscopy for medical applications: Current status and future perspectives. Clinica Chimica Acta, 455, pp. 181–188.

Baker M. J. (2014)
Using Fourier transform IR spectroscopy to analyze biological materials. Nature Protocols, 9, pp.1771–1791 doi:10.1038/nprot.2014.110

Qi J et al. (2009)
Raman spectroscopic study on Hela cells irradiated by x-rays of different doses. Chin. Opt. Lett. 7, pp. 734–737

Risi R., Manti L., Perna G., Lasalvia M., Capozzi V. , Lepore (2011)
Micro_Raman spetroscopy on human mammary epithelial cells irradiated by different doses of X-rays. IEEE Conf. 978-1-4244-9837-6/11

Matthews Q. et al. (2011)
Raman spectroscopy of single human tumour cells exposed to ionizing radiation in vivo. Phys. Med. Biol. 56,pp. 19–38.

Delfino I., Perna G., Lasalvia M., Capozzi V., Manti L., Camerlingo C., Lepore M. (2015)
Visible micro-Raman spectroscopy of single human mammary epithelial cells exposed to X-ray radiation. Journal of Biomedical Optics 20(3), 035003

Meade A., Clarke C., Byrne H., Lyng F(2010)
Fourier transform infrared microspectroscopy and multivariate methods for radiobiological dosimetry. Radiation Research, 173, pp. 225–237.